



# The synthesis strategy to enhance the performance and cyclic utilization of granulated activated carbon-based sorbent for bisphenol A and triclosan removal

Pamphile Ndagijimana<sup>1,2</sup> · Xuejiao Liu<sup>1</sup> · Zhiwei Li<sup>1</sup> · Guangwei Yu<sup>1</sup> · Yin Wang<sup>1</sup>

Received: 6 October 2019 / Accepted: 12 February 2020  
© Springer-Verlag GmbH Germany, part of Springer Nature 2020

## Abstract

For a potential and efficient solution in the mitigation of aquatic pollution, this study reported a well-designed and developed protected granulated activated carbon (GAC) material which ensures high strength property and adsorption performance to meet the industrial application. The prepared GAC material was shaped into a spherical core using natural binders basically assumed to constitute waste solids materials. Then after, the granulated carbon core (GAC core) was protected by a porous ceramic shell which confined the material with strong protection and high mechanical strength to resist against degeneration and pressure drop as a limiting factor for most sorbents employed in solution. The CSGAC characterization results proved that the ceramic shell has a smaller thickness (0.1 cm), good mechanical strength (2.0 MPa), and additionally, it presents larger porous channels which promote the fast and higher adsorption performance making it the desired material for the application in the real liquid environment. The test results showed that the prepared material had higher removal of triclosan (TCS) (30–40 mg/L) than BPA counterpart from the aqueous solutions. Moreover, it showed higher adsorption performance compared to the unprotected carbon materials. Furthermore, the mechanisms of BPA and TCS adsorption by core-shell granulated activated carbon (CSGAC) were discussed.

**Keywords** Adsorption · Bisphenol A · Granulated activated carbon · Porous ceramic shell · Triclosan

## Introduction

The aquatic environment is of a fundamental utility to sustain animals and plants lives; however, it has become the primary recipient channel for direct contamination of a group of chemicals known as emerging contaminants.

Since the industrialization era, pollutants constitute a menace to water environment including its habitants and terrestrial populations. Simple puzzle facing government, environmental agencies, and scientist communities is how to permanently solve this issue by designing a sustainable process without further secondary effects. The alternative and promising solution is to meet the desired level of equilibrium between industrial production and the need for a safe and secure environment. For example, on daily basis, disinfectants such as triclosan (TCS) is an antimicrobial classified into emerging organic contaminants (EOCs) commonly used in numerous commercial products such as shampoos, toothpaste, detergent, deodorants, body washes, lotions, and dishwashing liquids (Behera et al. 2010; Xie et al. 2018). Furthermore, it is a common additive in polymer, plastics, as well as in the textile manufacturing industry (Behera et al. 2010). These products are hydrophobic, have low solubility, and direct contact with water for their daily use (Dann and Hontela 2011; Khraisheh et al. 2014). Thus, they could be easily discharged into the water environment if not treated or completely removed from the treatment plant (Fiss et al. 2007; Thompson et al. 2005).

---

Responsible editor: Tito Roberto Cadaval Jr

**Electronic supplementary material** The online version of this article (<https://doi.org/10.1007/s11356-020-08095-7>) contains supplementary material, which is available to authorized users.

✉ Guangwei Yu  
gwyu@iue.ac.cn

✉ Yin Wang  
yinwang@iue.ac.cn

<sup>1</sup> CAS Key Laboratory of Urban Pollutant Conversion, Institute of Urban Environment, Chinese Academy of Sciences, Xiamen 361021, China

<sup>2</sup> University of Chinese Academy of Sciences, Beijing 100049, China

In the worst cases, TCS byproducts are probably more tolerant to degradation than its molecular form (parent) (Dann and Hontela 2011) and could also mutate into dioxin and endocrine-disrupting chemicals (EDCs) in drinking water and wastewater (Buth et al. 2010) which could be toxic to aquatic organisms. EDCs are other kinds of water pollutants that arouse the world concern owing to their immense presence in the aquatic ecosystem as well as harmful effect to human beings (Jung et al. 2015; Katsigiannis et al. 2015). EDCs are very dangerous to animals and humans due to their ability to mimic the biological activity of natural hormones in living things (Batra et al. 2019; Joseph et al. 2011). A common representative organic contaminant among EDCs, bisphenol A, has persistence features in the aquatic environment and in human beings (Calafat et al. 2005; Calafat et al. 2008). BPA is widely applied in plastics industries (Kabir et al. 2015; Fenichel et al. 2013) easily discharged in the environment sourcing from industrial effluents and wastewater treatment plant (Koduru et al. 2016).

Many technologies have been introduced for controlling the contaminant accumulation in the aquatic environment, but they are not enough efficiently to eliminate these unwanted substances. This drives the scientific communities to consider other alternative methods or improve the existing techniques which would be more efficient and industrially operational. For instance, it is well-known that the adsorption based on the activated carbon is a powerful method to mitigate organic pollutants in water environment (Alves et al. 2019; Kong et al. 2017), but applying powder or granules forms of carbon limit the application because of low recovery and reusability (Bayer et al. 2005; Guo and Du 2012). It was reported that during the regeneration process, there is a likely degeneration and gradual loss of adsorption properties and the carbon structure of granulated activated carbon (Guo and Du 2012). The estimation showed that the amount of carbon equivalent to 10–12% of the total GAC mass would be needed to substitute that one lost during regeneration, which exemplifies 20–40% of the price of GAC regeneration (Jeswani et al. 2015; Lambert et al. 2002). Conclusively, it would be nearly impossible to recover the full activated carbon during the regeneration process due to the diminution of intensity and size of the carbon, resulting into an increased loss of the mass (Lambert et al. 2002). One of the innovative ideas to make this technique feasible and more efficient would be to protect the GAC in a form which could protect the material from degradation and enhance its recovery and reusability to avoid left waste materials production, their ultimate disposal, and carbon losses with each subsequent cycle. Interested by the adsorption technology carbon-based material in the line of mitigation of pollution, our group has proposed and designed a protective material to enhance the property of the carbon adsorbent with the expectation to meet high-quality material to meet the application, regeneration, and reusability demands in a real liquid environment (Ndagijimana et al. 2019a; Ndagijimana

et al. 2019b). According to our recent studies, it was demonstrated that using a big particle size (100 mesh) of kaolinite (KL) and coal fly ash (CFA) mixture could produce the shell with wide intraparticle space which favored an easy mass transfer of adsorbate and increased the adsorption efficiency on inner AC core. However, it was also found that a part of the AC core derived from PAC could be generated and released out from the shell into the solution during the adsorption process. Thus, using GAC with precise size as AC core can ensure higher adsorption performance without AC releasing out during the adsorption process. Therefore in this work, the following works were carried out to address the aforementioned limitations: (i) synthesis of core-shell GAC (CSGAC) with the shell of suitable mechanical strength, small shell thickness, and large porous channel as new strategy to enhance the adsorption performance of material; (ii) its application to adsorb bisphenol A and triclosan from water matrix; and (iii) discussing the adsorption mechanisms as well as the kinetics and isotherm study.

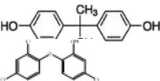
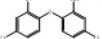
## Materials and methods

The materials used in this work were illustrated in supplementary material text S1. The structure and physical-chemical properties of BPA and TCs were presented in Table 1.

### Preparation and characterization of CSGAC

Figure 1 presents the procedure for the preparation of CSGAC. The three GAC cores were prepared by mixing the 0.45 mm, 0.9 mm, and 2.0 mm of GAC with the cassava splinters binder (CSB) by the proportions of 85%:15% (Table 2), and then, the sample was pelletized and dried at 105 °C for 2 h, named as GAC cores1 (Fig. 2a–c). The porous structure of the shell was formulated from a proportional mixing amount of 60% KL and 40% CFA, 100–100 meshes of particle size and then mixed with a certain amount of water. Finally, 0.4 g of the resulting mixture was wrapped on the prepared GAC core1 to form a protective shell of the core pellets namely CSGAC1, CSGAC2, and CSGAC3. The materials were dried at 105 °C and heated at 1250 °C under nitrogen flow, then after cooled at 25 °C (Fig. 1). The mechanical strength and the adsorption test (Fig. 2d) of the samples were evaluated in order to select the suitable material which could be used in this experiment. The CSGAC3 with 0.28 g was selected as suitable adsorbent due to its high adsorption performance and further characterizations were performed. The detailed procedure for producing CSGAC was explained according to previous work (Ndagijimana et al. 2019a) and Fig. 1. Furthermore, the equipment and operational mode of characterizations were given in supplementary material text S2.

**Table 1** The structure and physicochemical properties of BPA and TCs

Pollutants	Formula <sup>a</sup>	Structure <sup>b</sup>	Molecular weight <sup>b</sup>	Water solubility (mg/L) <sup>b</sup>	Melting point (°C)	Boiling point (°C)	pKa <sup>b</sup>	logKow <sup>b</sup>
Bisphenol A	C <sub>15</sub> H <sub>16</sub> O <sub>2</sub>		228.29	120	158–159	220	9.6–10.2	3.32
Triclosan	C <sub>12</sub> H <sub>7</sub> Cl <sub>3</sub> O <sub>2</sub>		289.54	10	55–57	120	8.14	4.76

<sup>a</sup>(Cho et al. 2011; Li et al. 2015)

<sup>b</sup>(Cho et al. 2011; Behera et al. 2010; Lei et al. 2013; Wang et al. 2017)

**Batch adsorption test**

Batch adsorption test was carried out in a conical flask with 0.28 g of CSGAC in 50 mL of the adsorbates solution (100 mg/L) at 25 °C under shaking at 180 rpm for 24 h. A membrane 0.45 μm was used to filter and collect the supernatants before testing. Analytical details were given in Supplementary material text S3. The effects of pH were determined from an initial concentration of 100 mg/L at 25 °C of each adsorbate adjusted at pH values of 2.0, 4.0, 7.0, 9.0, and 12.0 by adding 0.01 mol/L NaOH or 0.01 mol/L HCl. In a set of separate experiments, five-set of initial concentrations (30, 40, 50, 80, and 100 mg/L) were selected for analytical investigation of the influence of initial concentration at pH 7. The initial concentration of 100 mg/L was employed to investigate the effect of the contact time. Sample solutions were taken at a defined time during the 500-min period. The effect of ionic strength was tested using different concentration of NaCl 0.01, 0.05, 0.08, 0.1, 0.3, and 0.5 mol/L. The thermodynamic study was evaluated at five temperatures of 25, 30, 35, 40, and 45 °C. The temperatures were measured by water bath shaker and were constant under automatically controlling. To evaluate the regeneration ability of adsorbents, the exhausted CSGAC was regenerated according to the previous study (Ndagijimana et al. 2019a). The kinetics and isotherm models (Lei et al. 2013; Wang et al. 2017) were investigated and detailed explanations were provided in Supplementary material text S4.

**Results and discussions**

**Selection of suitable adsorbent and characterization**

The mechanical strength was evaluated and the results (Fig. 2d) showed that the CSGAC1 had good mechanical strength with 2.45 MPa. This is probably due to the high cohesion force generated from the small intraparticle space in GAC core material. Figure 2e showed the adsorption performance of synthesized materials and the CSGAC3 showed good performance compared to its counterparts. It may be due to the large intraparticle space in GAC core with 2 mm which promoted the easy mass transport movement of adsorbates solution through the external to the inner surface of GAC core. Lower adsorption performance for CSGAC1 was explained by smaller internal spaces between particles in GAC core (0.45 mm) making difficult the mass transfer inside the inner surface of GAC core. The smaller size of this core (0.45 mm) is a limitation for the utilization because of the apparent fraction of GAC core released out at a high agitation speed during the adsorption. Although the CSGAC1 showed good mechanical strength, it showed the limitations in adsorption process such as low adsorption performance and releasing out some part of the GAC core during the adsorption process. Therefore, in this study, the CSGAC3 (referred to as CSGAC) was selected as suitable material and further characterization was performed. Finally, the material was applied in adsorption of the aforementioned contaminants from aqueous solution.

**Fig. 1** The procedure for preparing core-shell structure GAC

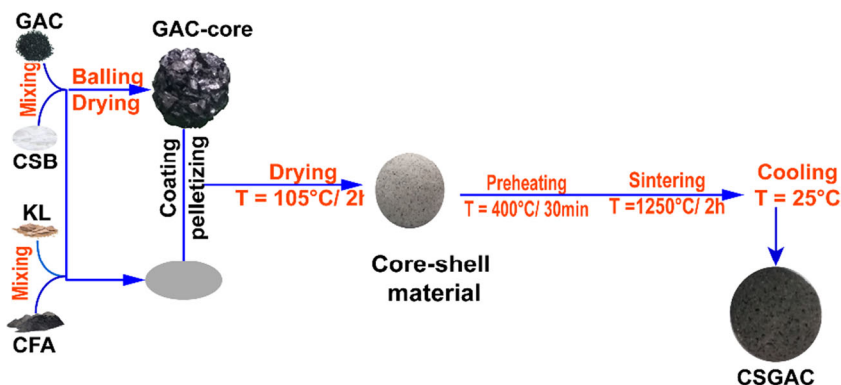


**Table 2** The proportion of raw materials used in the preparation of CSGAC

	Starting material	Proportion (%)	Size (mm)
Shell	KL	60	0.15
	CFA	40	0.15
GAC core	GAC	85	2.00
	CSB	15	0.74

Images of the sample prepared under optimal conditions were examined using SEM. Figure 3a showed the presence of porous on the ceramic shell sintered at 1250 °C. A big intraparticle void was observed on a porous ceramic shell made by K-CFA sieved at 100–100 meshes in Fig. 3b. The pore structures observed on the surface of GAC (Fig. 3c) were not developed well and differed from those of GAC core2 (referred to GAC core which separated from CSGAC after sintering at 1250 °C) which were more developed and wide because of the sintering effect of the samples at 1250 °C (Fig. 3d). The images of the GAC and the CSGAC were evidently and physically examined in Fig. 3e, f. The crystal phases of KL, CFA, and shell were analyzed by using XRD.

The dolomite, quartz, and diaspore were detected for CFA in addition to kaolinite mineral in KL (Fig. 4a). Figure 4b shows the XRD patterns of CSGAC (shell) from KL-CFA mixture after sintering at 1250 °C demonstrating the presence of mullite, anorthite, spinel, augite, and clinoenstatite. The mechanical strength of CSGAC was measured to a value of 2.0 MPa which is a high value to offer higher resistance of the material to degenerate and pressure drop in the filtration system. In fact, the presence of mullite, anorthite, spinel, augite, and clinoenstatite components could explain a higher mechanical strength bearing property of CSGAC. The reason of the decreasing and increasing of the  $S_{BET}$ , pore size, and pore volume of prepared materials as tabulated in Table 3 was explained in our previous work (Ndagijimana et al. 2019a; Ndagijimana et al. 2019b). Figure 5 depicted the pore size dispersion of the GAC, GAC core1, GAC core, CSGAC, KL-CFA, and shell of CSGAC. The corresponding curves of all adsorbents displayed broad trends of pore size distribution. GAC core1 and GAC displayed identical pore distribution characteristic showing the existence of micro- and mesopore owing to the intraparticle space (Fig. 5a). Clearly, the pore distribution curves for CSGAC and GAC core are wide, which explain the formation of large pore

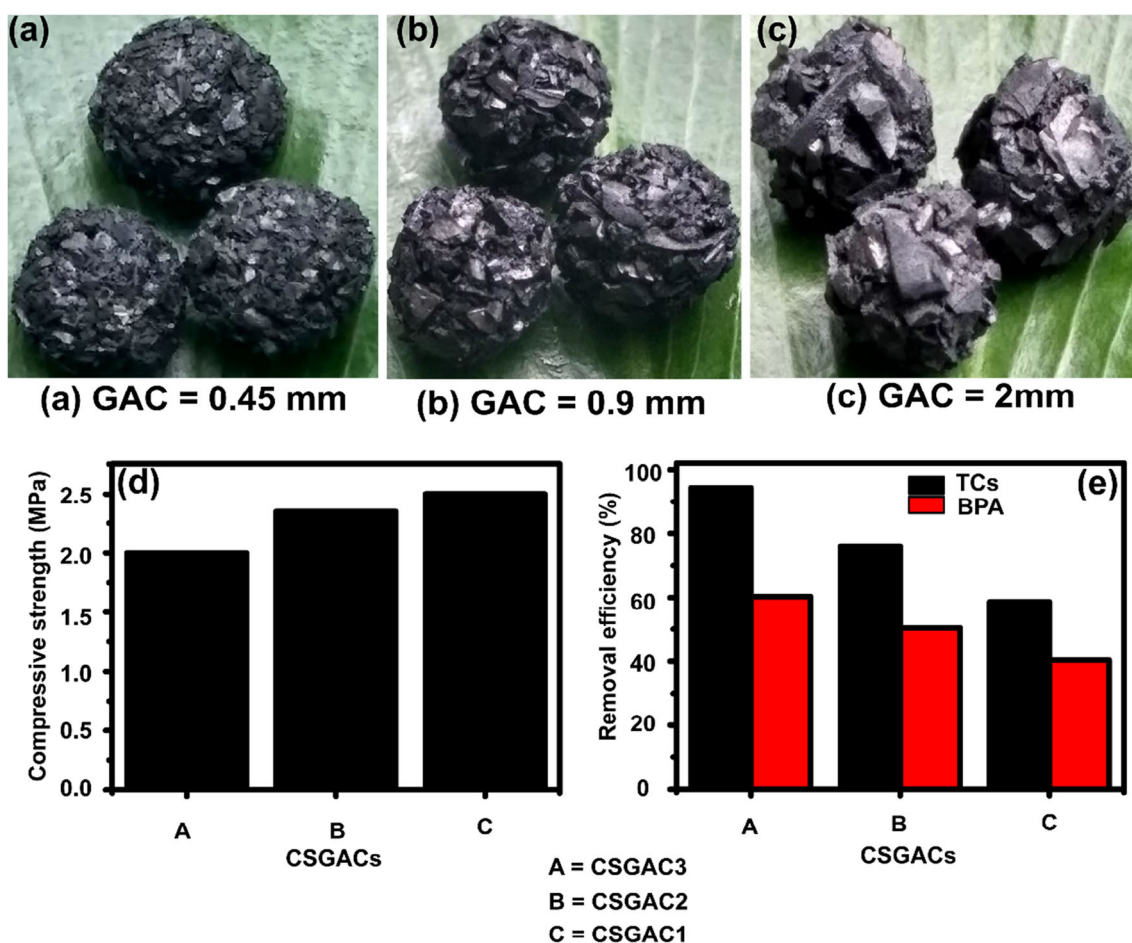
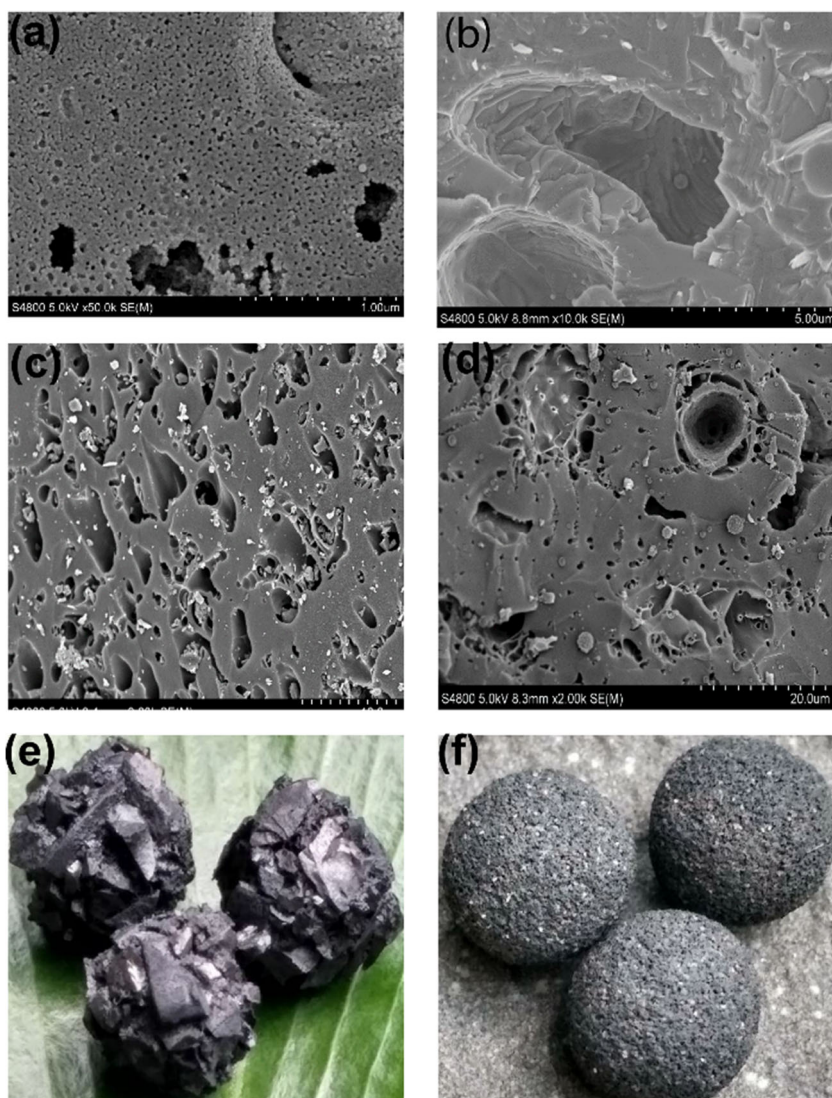


**Fig. 2** GAC cores with different size of GAC (a–c), compressive strength (d), and removal efficiency on different CSGAC (e)

**Fig. 3** SEM Morphology of ceramic shell surface (a, b), GAC (c), GAC core (d), the image of GAC core (e), and image of CSGAC (f)



sizes resulting from high-temperature effect (Fig. 5a, b). The pore size distribution for raw materials of the shell and CSGAC displayed the distribution of micropore, mesopore, and macropore (Fig. 5c, d). Now, the

increasing of the macropore distribution resulted from heating the material (Fig. 5d) would be one of the potential factors to favor and enhance the diffusion of the aforementioned adsorbates into CSGAC.

**Fig. 4** XRD patterns of coal fly ash and kaolinite (a) and ceramic shell (b)

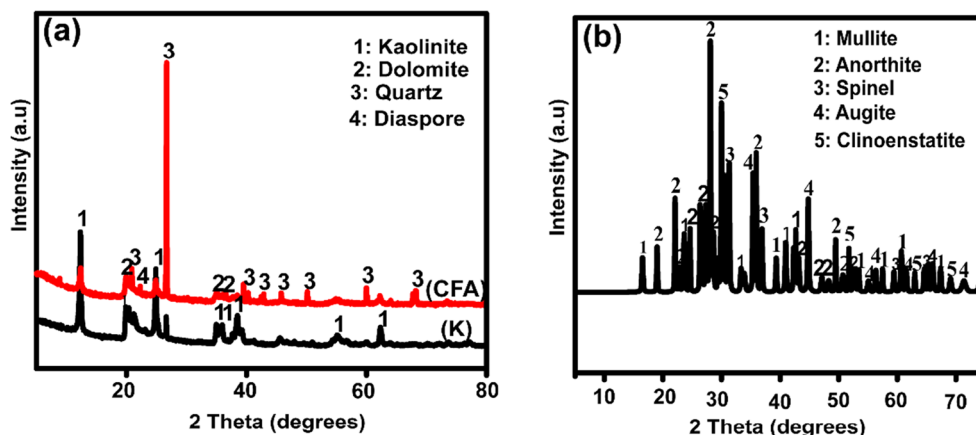


**Table 3** Surface area, pore volume, and pore size of materials

Sample	Surface area (m <sup>2</sup> /g)	Pore volume (cm <sup>3</sup> /g)	Pore size (nm)
GAC	510	0.28	2.20
GAC core1	462	0.25	2.20
GAC core 2	979	0.54	2.60
CSGAC	142	0.06	2.95
Shell	2	0.001	2.50
K-CFA	19	0.11	21.00
K	46	0.15	12.13
CFA	14	0.03	9.07

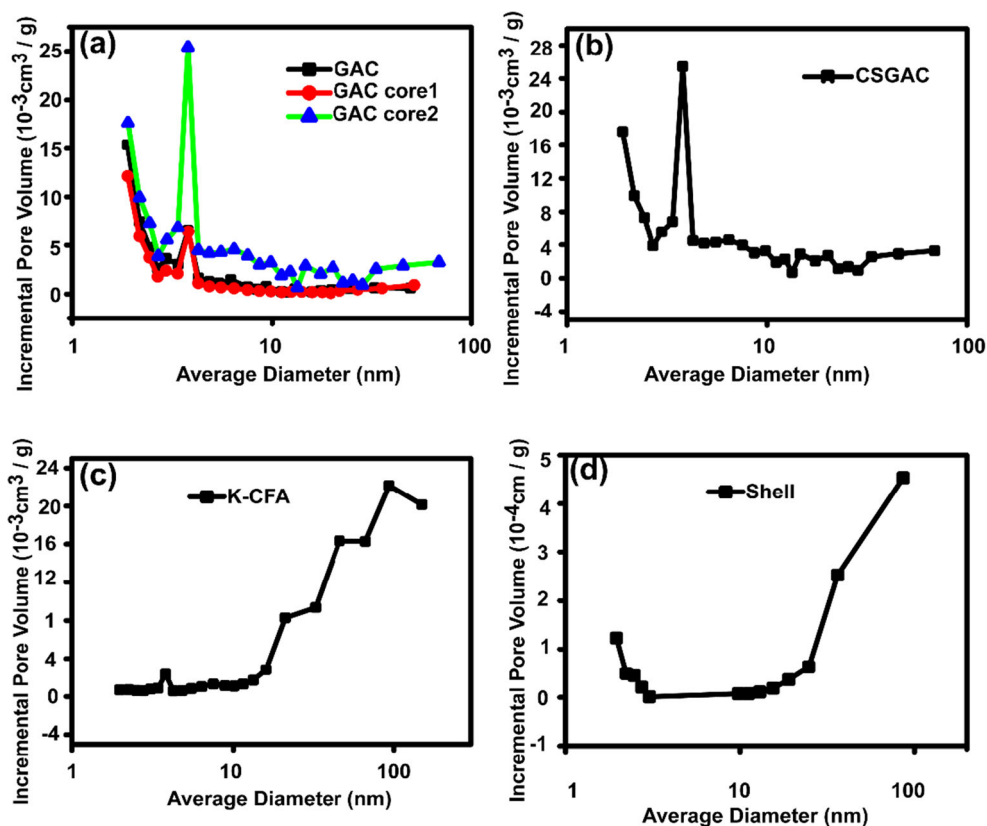
### Effect of initial pH

The effect of pH on the adsorption of the aforementioned adsorbates on CSGAC, GAC core, and GAC were presented in Fig. 6a, b. The zeta potential of the CSGAC powder suspension at different pH values (pHpzc = 1.66) was shown in Fig. 6c. From Fig. 6a, b, it can be seen that there was no significant effect on adsorption levels of both BPA and TCS at pH between 2.0 and 7.0. On the contrary, the adsorption decreased at pH value above 7.0 due to the formation of repulsive electrostatic interactions between anion adsorbent and adsorbate as explained in our previous study and Supplementary material text S5.

### Effect of initial concentration

The sorption of both BPA and TCS in solution was conducted with the dosage of 30, 40, 50, 80, and 100 mg/L. Analytical results evidenced that BPA solution was removed at 88, 71, 69, 63, and 60% respectively on CSGAC. Its removal efficiency was also 100, 100, 98, 91, 85, and 68, 66, 62, 52, and 48% on GAC core and GAC, respectively. At the same initial concentration, the CSGAC adsorbent showed the high removal efficiency of TCS, as it was clear that at 30 and 40 mg/L, TCS were totally removed, while for 50, 80, and 100 mg/L were removed at 99.0, 95.7, and 94.5% respectively. Similarly, lower concentrations of TCS (30 and 40 mg/L) also were totally removed on GAC core and GAC. Meanwhile, for higher concentrations, TCS were removed at 99.2, 98.6, 98.7 and 97.5, 92.8, and 90.9% on GAC core and GAC, accordingly. From Fig. 7a, b, the removal efficiency of both contaminants dropped with the initial concentration, which was contrary to the adsorption capacity slope. This observation matched well with other literature findings (Ndagijimana et al. 2019b; Tan et al. 2008). GAC core presented high removal efficiency probably due to its high surface area, big pore size, and big pore volume. Comparing with GAC, the high removal efficiency of CSGAC is due to the sintering of the material at a high temperature which causes the formation of macroporous on the outer shell and the increase of the pore size, pore volume into GAC core as well as breaking of some porous

**Fig. 5** Pore distribution for GAC, GAC core1 and GAC core 2 (a), core-shell GAC (b), KL-CFA raw materials of the shell (c), and shell after sintering at 1250 °C (d)



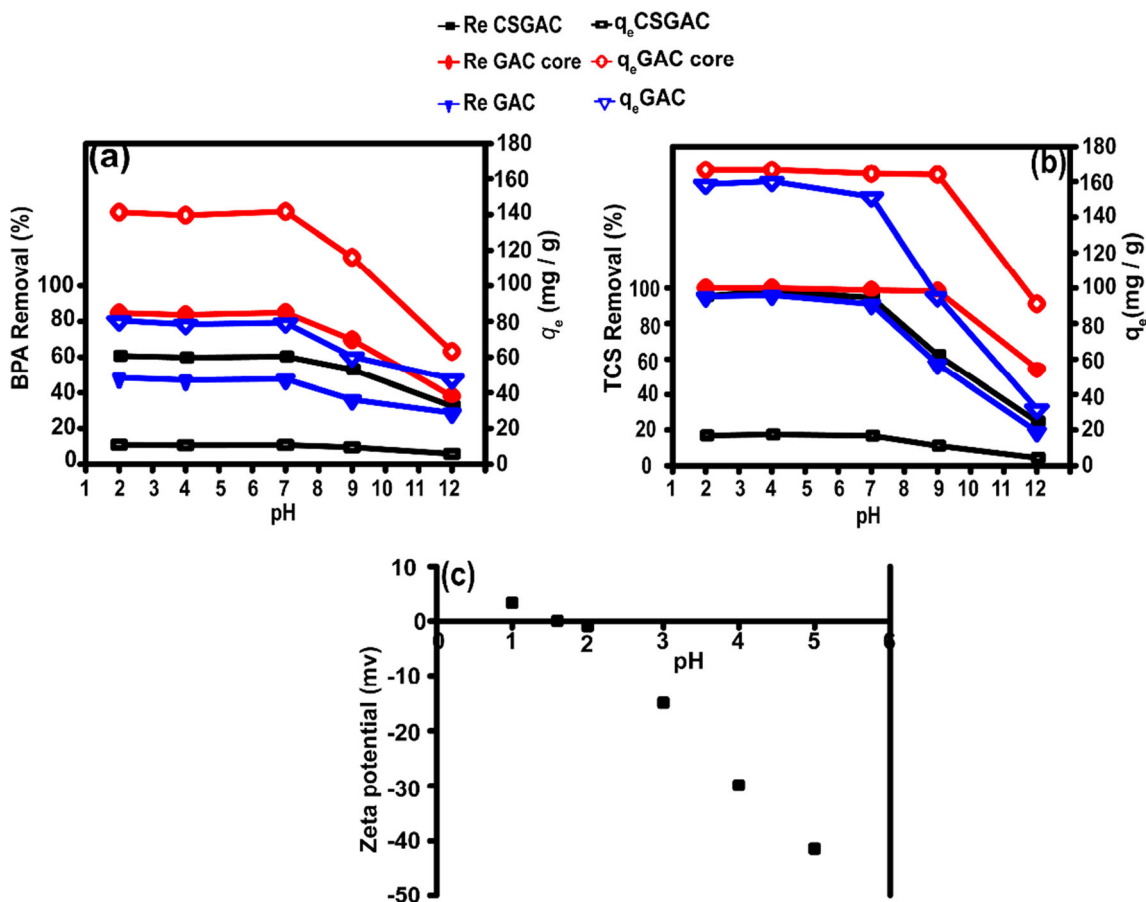


Fig. 6 Effects of pH (a, b) and zeta potential (c) on the adsorption of BPA and TCS

structure of the GAC core inside the shell. These properties formed after sintering of the CSGAC were the evidence of fast mass transport of solution through the shell and easily adsorbed into GAC core.

### Effect of ionic strength

We investigated the influence of ionic strength by using a solution of NaCl with different concentrations (0.01, 0.05, 0.08, 0.10, 0.30, and 0.50 mol/L). The ionic effect of the organic pollutant on porous adsorbent could be explained from three aspects such as salting-out, screening, and squeezing-out effect (Cui et al. 2016). Figure 7c showed that the adsorption capacity of BPA increased from 0.0 to 0.1 mol/L of NaCl because of screening effect of the surface charge and salting-out effect as explained above. The competitive adsorption between NaCl and BPA on the adsorbent sites could explain a decreasing of adsorption observed at higher concentrations of 0.1 to 0.5 mol/L NaCl attached to binding sites occupancy. Figure 7d illustrated that the concentration of NaCl had a slight effect on TCS adsorption. This could be explained by the hydrophobic

property of TCS which is higher than that of BPA (Table 1) to enhance its adsorption.

### Effect of contact time

From Fig. 8a, b, the study of contact time showed that the adsorption increased as a function of time to attain equilibrium between 420 and 480 min for CSGAC. Clearly, at first, the solution passed through the ceramic shell to reach the external surface of GAC core, followed by diffusion inside the internal surface of GAC core until the equilibrium is attained at about 480 min. In the same way, the adsorption process for GAC core separated from CSGAC followed the same patterns with a sharp increment and decrease to reach the equilibrium time of around 360 min. The removal rate of GAC core was higher than that of CSGAC and could be explained by the existence of the protective ceramic shell of the material, which decreased the mass transfer rate from the bulk solution and across the porous shell to the GAC core. The removal rates of BPA and TCS by GAC were faster than those of CSGAC and GAC core at the beginning and attained the equilibrium about 60 min; this could be associated with accessible binding sites and rapid diffusion of the solution through GAC.

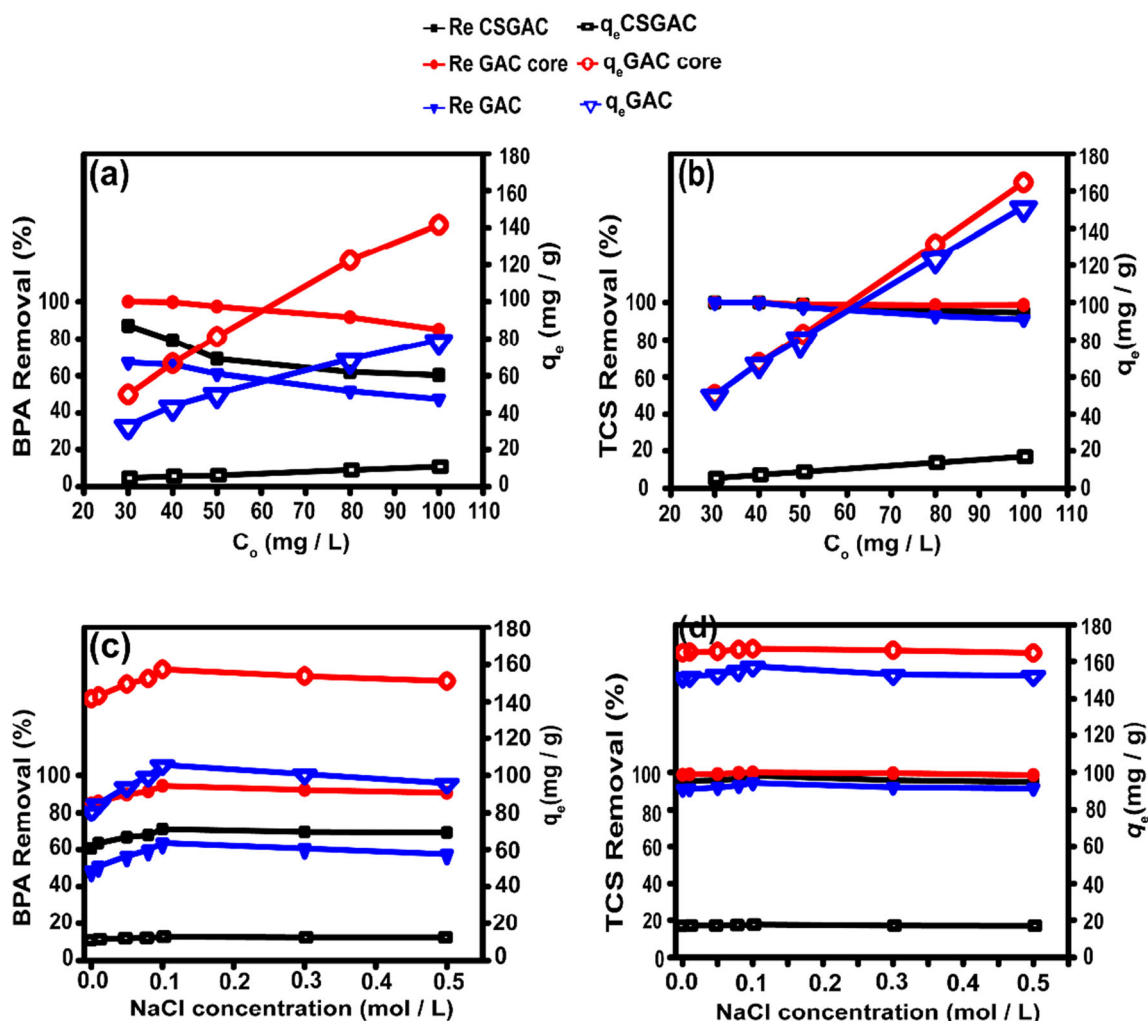


Fig. 7 Effects of initial concentrations (a, b) and NaCl ionic concentration (c, d) on sorption of BPA and TCS

### Regeneration test of CSGAC

As presented in Fig. 8c, d, the regeneration test was repeated six times following the same procedure and conditions proposed in our previous work (Ndagijimana et al. 2019a; Ndagijimana et al. 2019b). It can be seen that the regenerated CSGAC still had a good adsorption capability similar to the original CSGAC. Thus, protected granulated activated carbon material would be an ideal material for an application rather than unprotected GAC because the CSGAC retained its adsorption capacity at a long time of use (over the recycling cycle), whereas GAC presented the degeneration during regeneration as mentioned in the introduction.

### Adsorption kinetics

Table 4 presents the kinetic parameters and kinetics data for the pseudo-first-order and pseudo-second-order models. The pseudo-first-order model was dominated on BPA adsorption, while the pseudo-second-order model for TCS on CSGAC.

The analytical data proved that the pseudo-second-order was dominating for the sorption of BPA and TCs on GAC. Furthermore, adsorption on GAC core for BPA matched better with pseudo-first-order, whereas that of TCS coincided with pseudo-second-order. Detailed explanations of the kinetic study were provided in Supplementary material text S4.

### Adsorption isotherm

Table 5 illustrated the isotherm parameters data extracted from the Langmuir and Freundlich models where the measurements of  $q_m$  and  $K_L$  were calculated from the slope and intercept of a linear plot of  $C_e/q_e$  against  $C_e$  (Fig. 9a, b), to which the slope corresponded to  $1/q_m$  and intercept was equal to  $1/q_m K_L$ . The slope and intercept calculated from the plot of  $\ln q_e$  versus  $\ln C_e$  (Fig. 9c, d) gave the Freundlich constants ( $k_F$  and  $n$ ). The correlation coefficients ( $R^2$ ) values showed that the adsorption of studied adsorbates on CSGAC was dominant for both Langmuir and Freundlich. In contrast, Freundlich and Langmuir were much fitted on GAC core and GAC for TCS

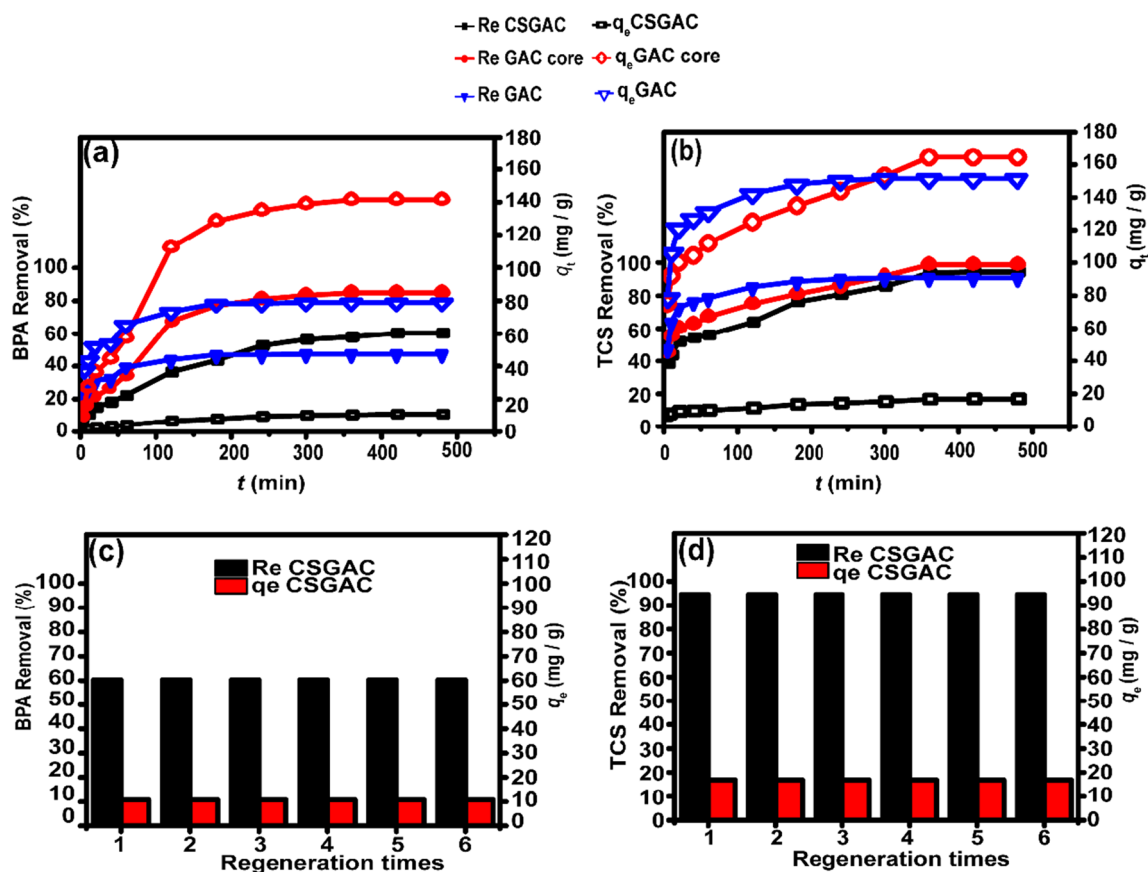


Fig. 8 Effects of contact time (a, b) and the regeneration times of CSGAC (c, d) on the removal of BPA and TCS

and BPA, respectively. The data analysis showed that the AC core had a higher adsorption capacity than GAC and CSGAC for both BPA and TCS adsorption. A possible reason for a lower adsorption capacity of CSGAC comparatively to GAC core might be the protective effect of the ceramic shell. Whereas, GAC core had significant adsorption capacity compared to the GAC (row material) because it was treated at a high temperature which enhanced an increment of the surface area. Comparative adsorption capacities of various sorbents used for adsorbing similar substances are given in Table 6. It is clear that the prepared materials (CSGAC and GAC core) had also good performance.

### Influence of temperature and thermodynamic study

The adsorption of organic pollutants onto CSGAC was studied at the different temperatures of 25, 30, 35, 40, and 45 °C. Figure 10a, b showed that the adsorption efficiency increased with the temperature, which implied it was an endothermic process. This was due to the increase of the adsorbates diffusion rate through the external boundary layer to the internal pores of core-shell GAC owing to the decrease of the viscosity of the adsorbates solution at high temperature. This indicated that the synthesized material will have a good adsorption performance in a real environmental condition at high

Table 4 The kinetic parameters of BPA and TCS adsorption

Sorbent	Sorbates	Pseudo-first-order				Pseudo-second-order				Intraparticle diffusion		
		$q_e^{exp}$ (mg/g)	$q_e^{calc}$ (mg/g)	$K_1$	$R^2$	$q_e^{exp}$ (mg/g)	$q_e^{calc}$	$K_2$	$R^2$	C	$K_{diff}$	$R^2$
CSGAC	BPA	10.76	10.67	$87 \times 10^{-3}$	0.984	10.76	12.73	$89 \times 10^{-4}$	0.973	0.35	0.52	0.973
	TCS	16.87	11.80	$88 \times 10^{-3}$	0.815	16.87	17.60	$17 \times 10^{-3}$	0.990	6.00	0.52	0.980
GAC core	BPA	141.60	147.20	$13 \times 10^{-2}$	0.993	141.60	167.20	$8 \times 10^{-5}$	0.982	17.80	6.40	0.956
	TCS	164.50	80.73	$60 \times 10^{-3}$	0.977	164.50	169.80	$24 \times 10^{-4}$	0.992	75.90	4.40	0.976
GAC	BPA	79.150	88.34	$18 \times 10^{-3}$	0.953	79.15	81.43	$17 \times 10^{-4}$	0.999	42.60	2.03	0.820
	TCS	151.48	54.00	$16 \times 10^{-2}$	0.976	151.48	155.50	$61 \times 10^{-4}$	0.999	101.0	2.80	0.930

**Table 5** The adsorption isotherm parameters of BPA and TCS adsorption

Sorbents	Sorbates	Langmuir isotherm			Freundlich isotherm		
		$q_m$ (mg/g)	$k_L$ (L/mg)	$R^2$	$k_F$ (mg/g)(L/mg) <sup>1/n</sup>	$n$	$R^2$
CSGAC	BPA	12.85	$65 \times 10^{-3}$	0.930	2.80	2.9	0.930
	TCS	16.54	$84 \times 10^{-4}$	0.970	10.03	3.5	0.970
GAC core	BPA	142.90	$23 \times 10^{-5}$	0.990	91.55	7.0	0.880
	TCS	156.70	$38 \times 10^{-6}$	0.914	134.60	2.0	0.933
GAC	BPA	110.62	$18 \times 10^{-3}$	0.995	11.90	2.0	0.978
	TCS	149.00	$18 \times 10^{-5}$	0.968	75.87	3.0	0.977

temperature. The Langmuir and Freundlich isotherm parameters were presented in Table 7. To better understand the adsorptive properties and temperature effects, the thermodynamic study (Supplementary information text S6) was evaluated. Figure 10c, d displays the obtained values and curves plotted by  $K_C$  against  $1/T$ . The value of the enthalpy ( $\Delta H^\circ$ ) was calculated to be positive (Table 8) which indicated an endothermic type of adsorption; thus, the adsorbate solution was orderly adsorbed on the surface of CSGAC. An estimation of  $\Delta G^\circ$  by Eq. 10 S6 gives values of energy tabulated in Table 8, thus the negative values would indicate a spontaneous adsorption reaction.

**Adsorption mechanism**

Figure 11 illustrated the possible adsorption mechanisms of BPA and TCS on CSGAC. The mechanisms were explained according to the pore structure of adsorbent and the nature of solution and adsorbates. The major transport processes included bulk transport, film transport intraparticle, and adsorption which takes place during the adsorption by a porous of the adsorbent. As a porous material, the adsorbates solution passed through the porous shell of CSGAC to the GAC core. Then the adsorbates reached the inner core (GAC core) through the external surface and diffused within intra-layers and internal pores of the GAC

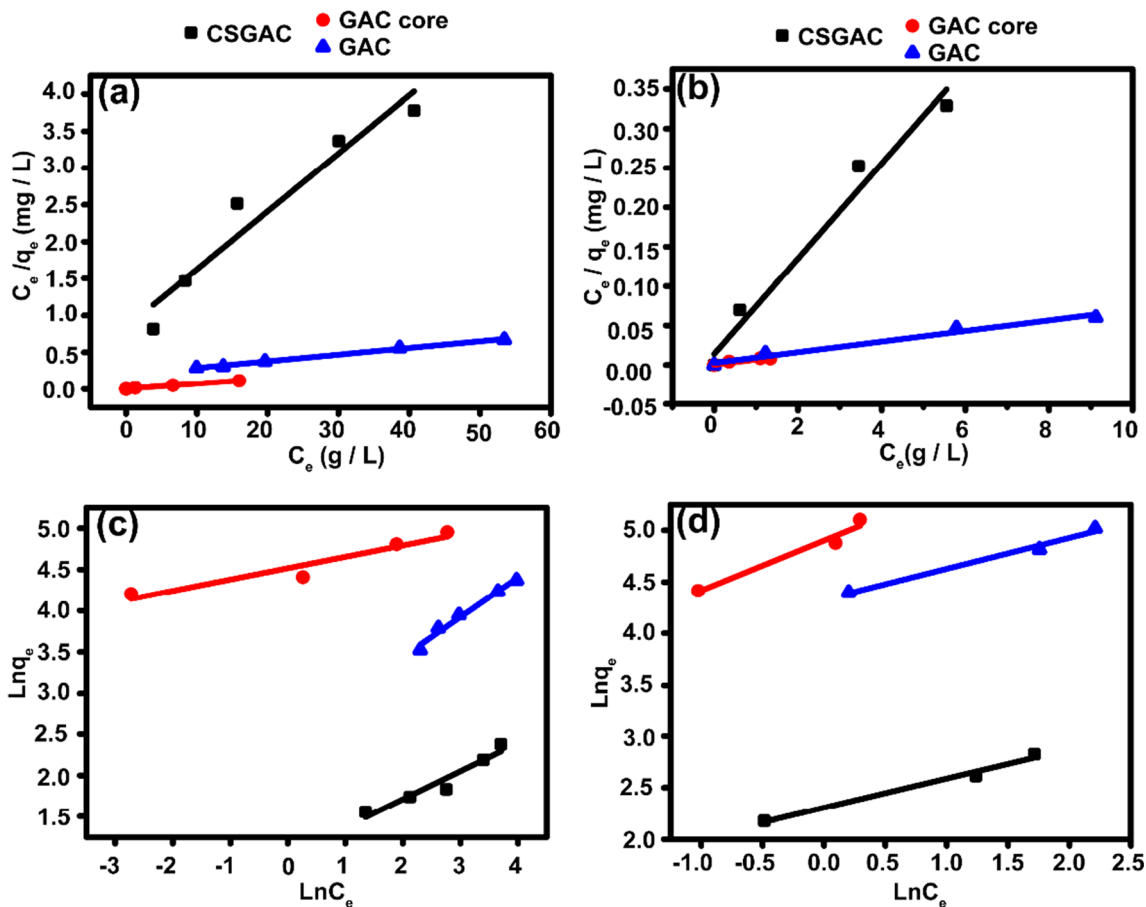


**Fig. 9** Langmuir model (a, b) and Freundlich model (c, d) for adsorption of BPA and TCS onto CSGAC, GAC core2, and GAC

**Table 6** Comparison of the adsorption capacity ( $q_m$ ) for BPA and TCS between various adsorbents

Pollutants	Adsorbents	$q_m$ (mg/g)	References
BPA	GAC	110.62	This work
	GAC core	142.90	This work
	CSGAC	12.85	This work
	Granular activated carbon	3.51	(Sudhakar et al. 2016)
	Rice Husk ash	8.72	(Sudhakar et al. 2016)
	10% CNTs/Fe <sub>3</sub> O <sub>4</sub>	44.40	(Li et al. 2015)
	AMBA Sericite	4.816	(Thanhmingliana and Tiwari Lee 2014)
	Aluminum AMBA Sericite	4.874	(Thanhmingliana and Tiwari Lee 2014)
TCS	CSGAC	16.54	This work
	GAC core	156.7	This work
	GAC	149.0	This work
	AC	67.11	(Behera et al. 2010)
	Kaolinite	6.03	(Behera et al. 2010)
	Organo-zeolites	49.65	(Lei et al. 2013)

core finally adsorbed onto micro-mesopore. The wide intraparticle space (Fig. 3b), destroyed pore structure due to the high temperature (Fig. 3d) and the increase of the  $S_{BET}$ , total pore

volume, micropore, and mesopore volumes of GAC core after sintering at 1250 °C (Table 3) were advantageous properties for the adsorption of BPA and TCS into the pores of GAC core. The

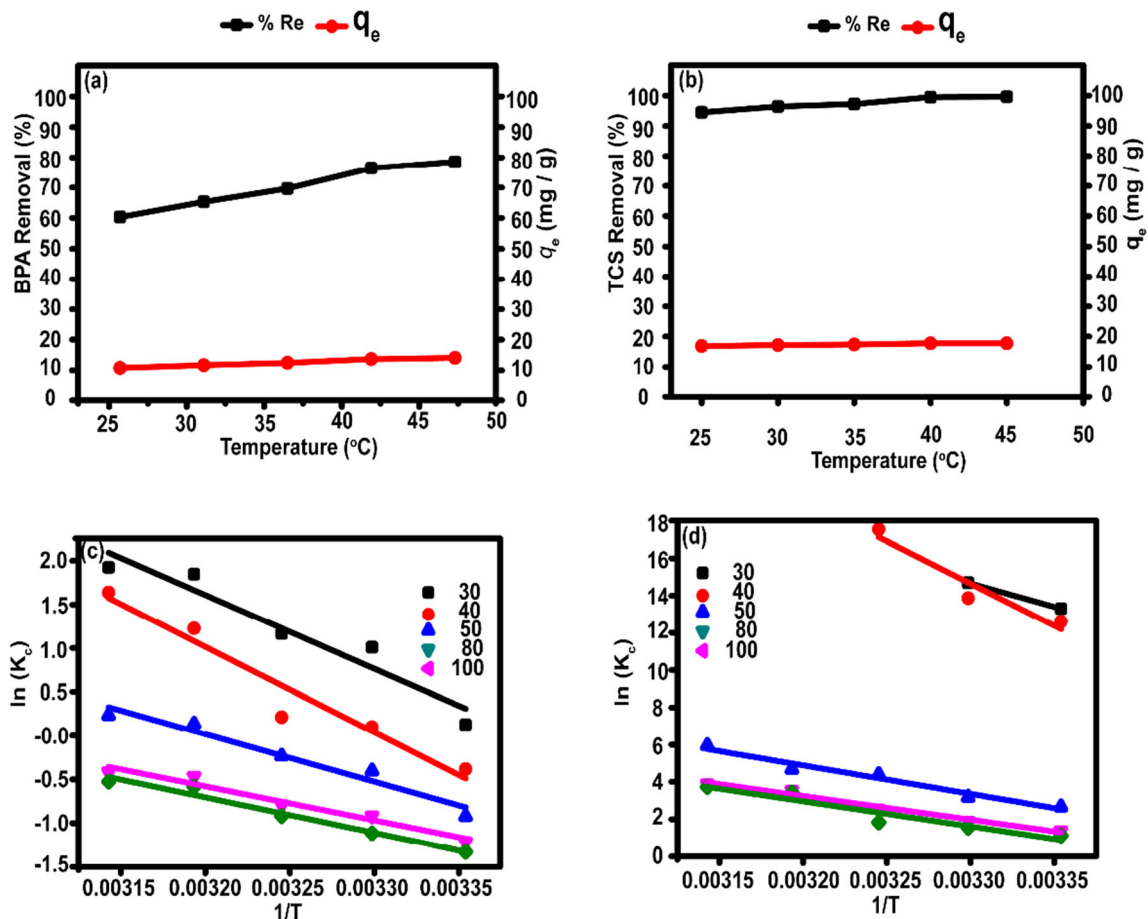


**Fig. 10** Temperature effect (a, b), plot of  $K_C$  versus  $1/T$  for determination of BPA, and TCS removal reaction enthalpy (c, d)

**Table 7** Effect of temperature on BPA and TCS adsorption

Isotherm	Temperature (°C)	Constant		
Langmuir		$q_{max}$ (mg/g)	$K_L$ (L/mg)	$R^2$
BPA	25	12.85	0.065	0.930
	30	12.91	0.035	0.961
	35	12.93	0.024	0.987
	40	13.75	0.012	0.918
	45	14.20	0.013	0.949
Freundlich	Temperature (°C)	Constant		
		$K_F$ (mg/g)(L/mg) <sup>1/n</sup>	$n$	$R^2$
BPA	25	2.80	2.90	0.930
	30	3.99	3.56	0.947
	35	4.14	3.00	0.941
	40	5.28	1.26	0.858
	45	5.80	4.00	0.906
Isotherm	Temperature (°C)	Constant		
Langmuir		$q_{max}$ (mg/g)	$K_L$ (L/mg)	$R^2$
TCS	25	16.54	$84 \times 10^{-4}$	0.970
	30	16.99	$5.0 \times 10^{-4}$	0.973
	35	16.99	$2.0 \times 10^{-4}$	0.988
	40	17.19	$97 \times 10^{-5}$	0.989
	45	17.42	$39 \times 10^{-5}$	0.9725
Freundlich	Temperature (°C)	Constant		
		$K_F$ (mg/g)(L/mg) <sup>1/n</sup>	$n$	$R^2$
TCS	25	10.03	3.5	0.970
	30	11.10	1.54	0.869
	35	13.43	3.60	0.895
	40	20.39	2.97	0.966
	45	20.40	4.00	0.921

microporous structure of carbon adsorbent was good at the texture of organic molecules such as BPA (Bautista-Toledo et al. 2005). As evidenced from Fig. 4c, d, all adsorbents were in the range of micropores (from 0 to 20 nm), thus all GAC adsorbents

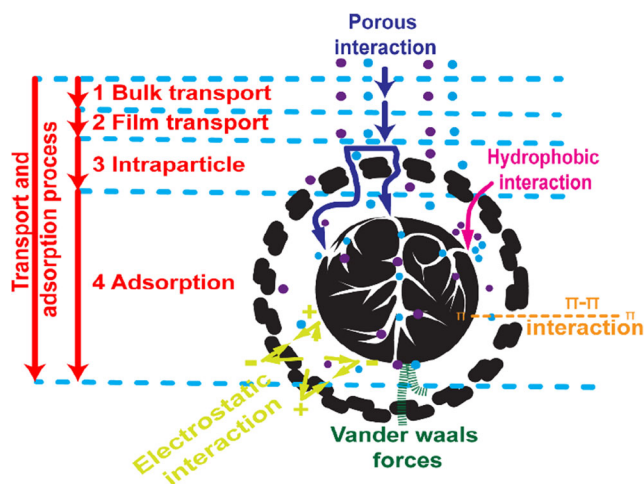


**Fig. 11** Possible adsorption mechanisms of BPA and TCS adsorbed on CSGAC

could remove BPA molecules from the water matrix. In addition, the interactions of pH of the solution, adsorbent surface  $pH_{pzc}$ , and  $pK_a$  of drugs could also affect the adsorption. Figure 6c showed that the  $pH_{pzc}$  value of CSGAC was 1.62. At a pH of 7, the CSGAC was positively charged, whereas BPA and TCS were in their molecular form (non-dissociated). Thus, the adsorption was promoted due to a minimization of repulsive electrostatic interactions and was probably enhanced by the existence of physicochemical interactions (Van der Waals,  $\pi$ - $\pi$ , and hydrophobic interactions), being consistent with those of other studies (Jun et al. 2019; Sun et al. 2017). According to the hydrophobicity measurement, the adsorption of organic molecules increased with the value of  $\log K_{ow}$  in octanol-water solution (Kaur et al. 2018; Wu et al. 2015; Wu et al. 2019). The hydrophobic interaction between TCs and CSGAC was much stronger than BPA due to its high  $\log K_{ow}$  (4.76) compared to that of BPA (3.32) (Table 1). Thus, the adsorption of TCS on adsorbent was highly moderated by existed hydrophobic and  $\pi$ - $\pi$  interactions in addition to textural properties of the synthesized material.

**Table 8** Thermodynamic study

Adsorbates	$C_o$ (mg/L)	$\Delta H$ (kJ/mol)	$\Delta S$ (J/mol/K)	$\Delta G$ (kJ/mol)				
BPA				298 K	303 K	308 K	313 K	318 K
	30	70.108	237.71	-0.334	-0.267	-3.075	-4.885	-5.087
	40	8.127	268.48	1.020	-0.260	-5.621	-3.237	-4.331
	50	45.122	144.52	2.442	1.070	0.612	-0.360	-0.619
	80	32.262	98.42	3.212	2.431	2.088	1.239	1.105
TCS	100	33.672	101.88	3.516	2.952	2.436	1.546	1.395
	30	208.347	809.38	-32.969	-37.016	-	-	-
	40	375.929	1362.28	-31.242	-34.963	-44.934	-	-
	50	126.690	446.01	-6.600	-8.028	-11.223	-12.180	-15.716
	80	105.359	364.13	-3.412	-4.773	-6.518	-9.250	-10.294
100	111.852	382.54	-2.756	-3.903	-4.699	-8.927	-9.868	

## Conclusions

A protective shell structure of core granulated carbon (CSGAC) with good properties desired for adsorbing EDCs was successfully synthesized. The material had a high mechanical strength (2.0 MPa) and small thickness (0.1 cm). This technique addressed a new and green technique to protect the GAC adsorbent with a ceramic shell which would ensure an easy utilization and recyclability of the material. The new (CSGAC) was successfully applied to remove bisphenol A and triclosan pollutants from aqueous solutions; the CSGAC exhibited higher efficiency in removing triclosan (TCS) than bisphenol A (BPA) from aqueous solutions and showed higher removal percentage for all adsorbates than GAC. The control of the textural pore structures and physicochemical interactions between adsorbent-adsorbate in solution ( $\pi$ - $\pi$  EDA, electrostatic, and hydrophobicity) is key to reach higher performance of the material and therefore, this material will play a great role in overcoming the existing limitation of applying GAC-based adsorbent in the liquid treatment-related applications.

**Acknowledgments** This research was supported by the Strategic Priority Research Program of the Chinese Academy of Sciences [Grant 467 No.XDA23030301, XDA23020500], China-Japan Research Cooperative Program [Grant No. 2016YFE0118000], the Natural Science Foundation of Fujian Province (2019J01135), the Science and technology program of Xiamen [3502Z20193076]; and support provided by CAS-TWAS President's Fellowship Program.

## References

- Alves ACF, Antero RVP, de Oliveira SB et al (2019) Activated carbon produced from waste coffee grounds for an effective removal of bisphenol-A in aqueous medium. *Environ Sci Pollut Res* 26: 24850–24862. <https://doi.org/10.1007/s11356-019-05717-7>
- Batra S, Datta D, Beesabathuni NS, Kanjolia N, Saha S (2019) Adsorption of Bisphenol-a from aqueous solution using Amberlite XAD-7 impregnated with Aliquat 336: batch, column, and design studies. *Process Saf Environ Prot* 122:232–246. <https://doi.org/10.1016/j.psep.2018.12.005>
- Bautista-Toledo BI, Ferro-Garcia MA, Rivera-Utrilla J, Moreno-Castilla C FFJV (2005) Bisphenol A removal from water by activated carbon. Effects of carbon characteristics and solution chemistry. *Environ Sci Technol* 39:6246–6250. <https://doi.org/10.1021/es0481169>
- Bayer P, Heur E, Karl U, Finkel M (2005) Economical and ecological comparison of granulated activated carbon (GAC) adsorbent refill strategies. *Water Res* 39:1719–1729. <https://doi.org/10.1016/j.watres.2005.02.005>
- Behera SK, Oh SY, Park HS (2010) Sorption of triclosan onto activated carbon, kaolinite and montmorillonite: effects of pH, ionic strength, and humic acid. *J Hazard* 179:684–691. <https://doi.org/10.1016/j.jhazmat.2010.03.056>
- Buth JM, Steen PO, Sueper C, Blumentritt D, Vikesland PJ, Arnold WA, McNeill K (2010) Dioxin photoproducts of triclosan and its chlorinated derivatives in sediment cores. *Environ Sci Technol* 44: 4545–4551. <https://doi.org/10.1021/es1001105>
- Calafat AM, Kuklennyik Z, Reidy JA, Caudill SP, Ekong J, Needham LL (2005) Urinary concentrations of bisphenol a and 4-nonylphenol in a human reference population. *Environ Health Perspect* 113:391–395. <https://doi.org/10.1289/ehp.7534>
- Calafat AM, Ye XY, Wong LY, ReidyJA NLL (2008) Exposure of the US population to bisphenol a and 4-tertiary-octylphenol: 2003–2004. *Environ Health Perspect* 116:39–44. <https://doi.org/10.1289/ehp.10753>
- Cho HH, Huang H, Schwab K (2011) Effects of solution chemistry on the adsorption of ibuprofen and Triclosan onto carbon nanotubes. *Langmuir* 27:12960–12967. <https://doi.org/10.1021/la202459g>
- Cui L, Wei J, Du X, Zhou X (2016) Preparation and evaluation of self-assembled porous microspheres—fiber for removal of bisphenol a from aqueous solution. *Ind Eng Chem Res* 55:1566–1574. <https://doi.org/10.1021/acs.iecr.5b04306>
- Dann AB, Hontela A (2011) Triclosan: environmental exposure, toxicity and mechanisms of action. *J Appl Toxicol* 31:285–311. <https://doi.org/10.1002/jat.1660>
- Fenichel P, Chevalier N, Brucker-Devis F (2013) Bisphenol a: an endocrine and metabolic disruptor. *Ann Endocrinol* 74:211–220. <https://doi.org/10.1016/j.ando.2013.04.002>
- Fiss EM, Rule KL, Vikesland PJ (2007) Formation of chloroform and other chlorinated byproducts by chlorination of triclosan-containing antibacterial products. *Environ Sci Technol* 41:2387–2394. <https://doi.org/10.1021/es062227f>
- Guo Y, Du E (2012) The effects of thermal regeneration conditions and inorganic compounds on the characteristics of activated carbon used in power plant. *Energy Proc* 17:444–449. <https://doi.org/10.1016/j.egypro.2012.02.118>
- Jeswani HK, Gujba H, Brown NW, Roberts EPL, Azapagic A (2015) Removal of organic compounds from water: life cycle environmental impacts and economic costs of the Arvia process compared to granulated activated carbon. *J Clean Prod* 89:203–213. <https://doi.org/10.1016/j.jclepro.2014.11.017>
- Joseph L, Zaib Q, Khan IA, Berge ND, Park YG, Saleh NB, Yoon Y (2011) Removal of bisphenol a and 17 alpha-ethinyl estradiol from landfill leachate using single-walled carbon nanotubes. *Water Res* 45:4056–4068. <https://doi.org/10.1016/j.watres.2011.05.015>
- Jun B-M, Hwang HS, Heo J, Han J, Jang M, Sohn J, Park CM, Yoon Y (2019) Removal of selected endocrine-disrupting compounds using Al-based metal organic framework: performance and mechanism of competitive adsorption. *J Ind Eng Chem* 79:345–352. <https://doi.org/10.1016/j.jiec.2019.07.009>
- Jung C, Son A, Her N, Zoh KD, Cho J, Yoon Y (2015) Removal of endocrine disrupting compounds, pharmaceuticals, and personal care products in water using carbon nanotubes: a review. *J Ind Eng Chem* 27:1–11. <https://doi.org/10.1016/j.jiec.2014.12.035>
- Kabir ER, Rahman S, Rahman I (2015) A review on endocrine disruptors and their possible impacts on human health. *Environ Toxicol Pharmacol* 40:241–258. <https://doi.org/10.1016/j.etap.2015.06.009>
- Katsigiannis A, Noutsopoulos C, Mantziaras J, Gioldasi M (2015) Removal of emerging pollutants through granular activated carbon. *Chem Eng J* 280:49–57. <https://doi.org/10.1016/j.cej.2015.05.109>
- Kaur H, Bansiwala A, Hippargi G et al (2018) Effect of hydrophobicity of pharmaceuticals and personal care products for adsorption on activated carbon: adsorption isotherms, kinetics and mechanism. *Environ Sci Pollut Res* 25:20473–20485. <https://doi.org/10.1007/s11356-017-0054-7>
- Khraishah M, Kim J, Campos L, Al-Muhtaseb AH, Al-Hawari A, Al Ghouti M et al (2014) Removal of pharmaceutical and personal care products (PPCPs) pollutants from water by novel TiO<sub>2</sub>-coconut Shell powder (TCNSP) composite. *J Ind Eng Chem* 20:979–987. <https://doi.org/10.1016/j.jiec.2013.06.032>

- Koduru JR, Lingamdinne LP, Singh J, Choo KH (2016) Effective removal of bisphenol-a (BPA) from water using a goethite/activated carbon composite. *Process Saf Environ Prot* 103:87–96. <https://doi.org/10.1016/j.psep.2016.06.038>
- Kong L, Su M, La PengY H, Liu J, Li H, Diao Z, Shih K, Xiong Y, Chen D (2017) Producing sawdust derived activated carbon by calcinations with limestone for enhanced acid Orange II adsorption. *J Clean Prod* 168:22–29. <https://doi.org/10.1016/j.jclepro.2017.09.005>
- Lambert SD, Miguel GS, Graham NJD (2002) Deleterious effects of inorganic compounds during thermal regeneration of GAC: a review. *J Am Water Works Assoc* 94:109–119. <https://doi.org/10.1002/j.1551-8833.2002.tb10253.x>
- Lei C, Hu Y-y, He M-z (2013) Adsorption characteristics of triclosan from aqueous solution onto cetylpyridinium bromide (CPB) modified zeolites. *Chem Eng J* 219:361–370. <https://doi.org/10.1016/j.cej.2012.12.099>
- Li S, Gong Y, Ynag Y, He C, Hu L, Zhu L, Shu D (2015) Recyclable CNTs/Fe<sub>3</sub>O<sub>4</sub> magnetic nanocomposites as adsorbents to remove bisphenol a from water and their regeneration. *Chem Eng J* 260: 231–239. <https://doi.org/10.1016/j.cej.2014.09.032>
- Ndagijimana P, Xuejiao L, Guangwei Y, Yin W (2019a) Synthesis of a novel core-shell-structure activated carbon material and its application in sulfamethoxazole adsorption. *J Hazard Mater* 368:602–612. <https://doi.org/10.1016/j.jhazmat.2019.01.093>
- Ndagijimana P, Xuejiao L, Zhiwei L, GuanweiY YW (2019b) Optimized synthesis of a core-shell structure activated carbon and its adsorption performance for Bisphenol a. *Sci Total Environ* 689:457–468. <https://doi.org/10.1016/j.scitotenv.2019.06.235>
- Sudhakar P, Mall ID, Srivastava VC (2016) Adsorptive removal of bisphenol a by rice husk ash and granular activated carbon – a comparative study. *Desalination Water Treat* 57:12375–12384. <https://doi.org/10.1080/19443994.2015.1050700>
- Sun W, Wang C, Pan W, Li S, Chen B (2017) Effects of natural minerals on the adsorption of 17 $\beta$ -estradiol and bisphenol a on graphene oxide and reduced graphene oxide. *Environ. Sci Nano* 4:1377–1388. <https://doi.org/10.1039/C7EN00295E>
- Tan IAW, Ahmad AL, Hameed BH (2008) Adsorption of basic dye on high-surface-area activated carbon prepared from coconut husk: equilibrium, kinetic and thermodynamic studies. *J Hazard Mater* 154:337–346. <https://doi.org/10.1016/j.jhazmat.2007.10.031>
- Thanhmingliana SM, Tiwari Lee D (2014) Use of hybrid materials in the decontamination of bisphenol a from aqueous solution. *RSC Adv* 4: 43921–43930. <https://doi.org/10.1039/C4RA06793B>
- Thompson A, Griffin P, Stuetz R, Cartmell E (2005) The fate and removal of triclosan during wastewater treatment. *Water Environ Res* 77:63–67. <https://doi.org/10.2175/106143005x41636>
- Wang F, Lu X, Peng W, Deng Y, Zhang T, Hu Y-B, Li XY (2017) Sorption behavior of bisphenol A and triclosan by graphene: comparison with activated carbon. *ACS Omega* 2:5378–5384. <https://doi.org/10.1021/acsomega.7b00616>
- Wu WJ, Hu YY, Guo Q, Yan J, Chen YC, Cheng JH (2015) Sorption/desorption behavior of triclosan in sediment-water-rhamnolipid systems: effects of pH, ionic strength, and DOM. *J Hazard Mater* 297: 59–65. <https://doi.org/10.1016/j.jhazmat.2015.04.078>
- Wu P, Cai Z, Jin H, Tang Y (2019) Adsorption mechanisms of five bisphenol analogues on PVC microplastics. *Sci Total Environ* 650: 671–678. <https://doi.org/10.1016/j.scitotenv.2018.09.049>
- Xie HJ, Yang YX, Liu JH, Kang Y, Zhang J, Hu Z, Liang S (2018) Enhanced triclosan and nutrient removal performance in vertical up-flow constructed wetlands with manganese oxides. *Water Res* 143:457–466. <https://doi.org/10.1016/j.watres.2018.05.061>

**Publisher's note** Springer Nature remains neutral with regard to jurisdictional claims in published maps and institutional affiliations.